

This is a repository copy of *The Decoupled Mind : Mind-wandering Disrupts Cortical Phase-locking to Perceptual Events*.

White Rose Research Online URL for this paper:

<https://eprints.whiterose.ac.uk/91766/>

Version: Submitted Version

---

**Article:**

Baird, Benjamin, Smallwood, Jonathan [orcid.org/0000-0002-7298-2459](https://orcid.org/0000-0002-7298-2459), Lutz, Antoine et al. (1 more author) (2014) *The Decoupled Mind : Mind-wandering Disrupts Cortical Phase-locking to Perceptual Events*. *Journal of Cognitive Neuroscience*. pp. 2596-2607. ISSN 0898-929X

[https://doi.org/10.1162/jocn\\_a\\_00656](https://doi.org/10.1162/jocn_a_00656)

---

**Reuse**

Items deposited in White Rose Research Online are protected by copyright, with all rights reserved unless indicated otherwise. They may be downloaded and/or printed for private study, or other acts as permitted by national copyright laws. The publisher or other rights holders may allow further reproduction and re-use of the full text version. This is indicated by the licence information on the White Rose Research Online record for the item.

**Takedown**

If you consider content in White Rose Research Online to be in breach of UK law, please notify us by emailing [eprints@whiterose.ac.uk](mailto:eprints@whiterose.ac.uk) including the URL of the record and the reason for the withdrawal request.

**Regional white matter variation associated with domain-specific metacognitive accuracy**

Journal:	<i>Journal of Cognitive Neuroscience</i>
Manuscript ID:	JOCN-2014-0228.R1
Manuscript Type:	Original
Date Submitted by the Author:	n/a
Complete List of Authors:	Baird, Benjamin Cieslak, Matthew; University of California, Santa Barbara, Department of Psychological and Brain Sciences Smallwood, Jonathan Grafton, Scott; University of California, Santa Barbara, Department of Psychological and Brain Sciences Schooler, Jonathan; University of California, Santa Barbara,
Keywords:	Consciousness, Decision making

1  
2  
3  
4  
5  
6  
7  
8  
9  
10  
11 Regional white matter variation associated with domain-specific metacognitive accuracy  
12  
13  
14  
15  
16  
17  
18  
19  
20  
21  
22  
23  
24  
25  
26  
27  
28  
29  
30  
31  
32  
33  
34  
35  
36  
37  
38  
39  
40  
41  
42  
43  
44  
45  
46  
47  
48  
49  
50  
51  
52  
53  
54  
55  
56  
57  
58  
59  
60

Benjamin Baird<sup>1</sup>

Matthew Cieslak<sup>1</sup>

Jonathan Smallwood<sup>2</sup>

Scott T. Grafton<sup>1</sup>

Jonathan W. Schooler<sup>1</sup>

<sup>1</sup>Department of Psychological and Brain Sciences  
University of California, Santa Barbara

<sup>2</sup>Department of Psychology / York Neuroimaging Centre.  
University of York, England

Address for correspondence: Benjamin Baird, Department of Psychological and Brain  
Sciences • University of California, Santa Barbara, CA 93106-9660

Email: [baird@psych.ucsb.edu](mailto:baird@psych.ucsb.edu)

**Abstract**

The neural mechanisms that mediate metacognitive ability (the capacity to accurately reflect on one's own cognition and experience) remain poorly understood. An important question is whether metacognitive capacity is a domain-general skill supported by a core neuroanatomical substrate or whether regionally specific neural structures underlie accurate reflection in different cognitive domains. Providing preliminary support for the latter possibility, recent findings have shown that individual differences in metacognitive ability in the domains of memory and perception are related to variation in distinct gray matter volume and resting-state functional connectivity. The current investigation sought to build on these findings by evaluating how metacognitive ability in these domains is related to variation in white matter microstructure. We quantified metacognitive ability across memory and perception domains and used diffusion spectrum imaging to examine the relation between high-resolution measurements of white matter microstructure and individual differences in metacognitive accuracy in each domain. We found that metacognitive accuracy for perceptual decisions and memory were uncorrelated across individuals and that metacognitive accuracy in each domain was related to variation in white matter microstructure in distinct brain areas. Metacognitive accuracy for perceptual decisions was associated with increased diffusion anisotropy in white matter underlying the anterior cingulate cortex, whereas metacognitive accuracy for memory retrieval was associated with increased diffusion anisotropy in the white matter extending into the inferior parietal lobule. Together, these results extend previous findings linking metacognitive ability in the domains of perception and memory to variation in distinct brain structures and connections.

## Introduction

Metacognition refers to reflection on or analysis of one's own cognitive processes. The ability "to doubt what one knows, to deny or affirm one's beliefs, to judge one's own memories and percepts, to comment on one's dreams, to recollect and reflect on one's own past" (Terrace & Metcalf, 2004, p. 2) represent several of the core abilities commonly referred to under the umbrella term of metacognition (Metcalf & Shimamura, 1994). Metacognition may be viewed as a general category that encompasses these processes, as well as introspection, which has been proposed to be a special case of metacognition involving specifically conscious content as the object of reflection (Fleming, Dolan, & Frith, 2012; Overgaard & Sandberg, 2012). However, metacognition appears to be distinct from other potentially related constructs such as intelligence, as individual differences in metacognitive ability are uncorrelated with general fluid intelligence (*g*) (Fleming, Huijgen, & Dolan 2012).

Despite the seeming immediacy with which we reflect on our minds, a central insight that has emerged from research in the cognitive sciences over the past forty years is that our access to our minds is noisy and subject to inaccuracies and dissociations (e.g., Schooler & Schreiber, 2004; Schooler, 2002). Metacognitive awareness is particularly compromised for causal-explanatory theorizing about the reasons for actions or decisions (Gazzaniga & LeDoux, 1978; Hall, Johansson, Tärning, Sikström, & Deutgen, 2010; Johansson, Hall, Sikström, & Olsson, 2005; Nisbett & Wilson, 1977). For example, classic studies revealed that individuals whose choice preferences are biased through priming or position effects are generally unaware of these effects and confabulate reasons for their selections (Nisbett & Wilson, 1977). Other research has illustrated the frequent dissociations that occur in metacognitive monitoring of the ongoing state of one's mind. One striking (and perhaps relatable) example is that individuals often fail to notice that their minds have wandered to unrelated topics during reading or sustained attention tasks, even in the context of experiments in which they are specifically instructed to remain vigilant for such lapses and report them as soon as they occur (Christoff, Gordon, Smallwood, Smith, & Schooler, 2009; Schooler, Reichle, & Halpern, 2004; Schooler et al., 2011; Smallwood, McSpadden, & Schooler, 2008).

The cognitive and neural mechanisms that mediate the fidelity of metacognitive awareness remain poorly understood. Recent research has exploited individual differences in metacognitive accuracy in healthy individuals as one approach to elucidating the neural mechanisms underlying the capacity to accurately reflect on particular cognitive processes (Baird, Smallwood, Gorgolewski, & Margulies, 2013; Fleming, Weil, Nagy, Dolan, & Rees, 2010; McCurdy et al., 2013). These studies converge with prior work in documenting a primary role of prefrontal cortex in metacognition, particularly the anterior PFC (see Fleming & Dolan, 2012 for a review). However, it remains equivocal whether metacognitive ability is a domain-general skill supported by a single neuroanatomical substrate or whether it varies across different processes or cognitive domains. On the one hand, the fact that metacognition has been linked to a "higher-order" brain region in PFC might suggest that it is supported by brain mechanisms that supersede cognition-level processing in a given domain, supporting a domain-general rather than domain-specific account (Song et al., 2011). On the other

1  
2  
3 hand, if metacognitive ability depends on the integration between PFC and cognition-  
4 level processing, it is also plausible that multiple brain networks linking domain-specific  
5 processing in posterior regions to frontal cortex could underlie metacognitive capacity in  
6 a particular domain (Nelson & Narens, 1990; Shimamura, 2000).  
7

8 Patient populations display greater impairment for some types of metacognitive tasks  
9 compared to others, potentially because they are supported by distinct neural structures.  
10 For instance, schizophrenic patients appear to have a relatively preserved capacity to  
11 make retrospective metacognitive judgments of their memory as well as trial-by-trial  
12 judgments of their performance accuracy, despite showing significant impairment in  
13 metacognitive judgments of their own agency as well as a generalized impairment in  
14 insight into their disorder (David, Bedford, Wiffen, & Gilleen, 2012; Metcalfe, Van  
15 Snellenberg, DeRosse, Balsam, & Malhotra, 2012). Furthermore, preliminary studies in  
16 healthy individuals have suggested that there may be domain-specificity in the neural  
17 basis of metacognitive ability in distinct cognitive domains. Specifically, two recent  
18 studies found that individuals' metacognitive accuracy in perception and memory tasks  
19 were related to differential neural substrates. McCurdy et al. (2013) found that gray  
20 matter volume in the distinct regions of the lateral aPFC and precuneus covaried with  
21 metacognitive accuracy in perception and memory domains, respectively. Furthermore,  
22 Baird et al. (2013) found that individual differences in metacognitive accuracy in each  
23 domain were associated with resting-state functional connectivity in distinct brain  
24 networks. Metacognitive accuracy for perceptual decisions was linked to greater  
25 connectivity between lateral aPFC and the right dorsal anterior cingulate cortex (dACC)  
26 and dorsal striatum, whereas metacognitive accuracy for memory retrieval was related to  
27 greater connectivity between medial aPFC and the right precuneus and inferior parietal  
28 lobule (IPL).  
29  
30  
31  
32

33 In the current investigation, we sought to build on these findings by evaluating how  
34 metacognitive ability in perceptual and mnemonic domains is related to individual  
35 differences in anatomical connectivity strength. We first quantified metacognitive  
36 accuracy in perception and memory domains and assessed intra-individual covariance in  
37 metacognitive accuracy. We then used diffusion spectrum imaging (DSI) (Schmahmann  
38 et al., 2007; Wedeen, Hagmann, Tseng, Reese, & Weisskoff, 2005) to examine the  
39 relation between high-resolution measurements of white matter microstructure and  
40 individual differences in metacognitive accuracy for perceptual decisions and mnemonic  
41 judgments. Most previous studies examining the relationship between cognitive abilities  
42 and variation in white matter anatomy have relied on the diffusion tensor model, and  
43 specifically averaged fractional anisotropy (FA), which is limited in its ability to model  
44 the crossing-fiber architecture of white matter that is ubiquitous in the brain (Jones,  
45 Knösche, & Turner, 2013). Specifically, DTI significantly underestimates the actual  
46 distribution of fiber pathways and can be inaccurate in regions of partial volumes of  
47 cerebrospinal fluid or gray matter (Alexander, Hasan, Lazar, Tsuruda, & Parker, 2001;  
48 Oouchi et al., 2007; Vos, Jones, Viergever, & Leemans, 2011). In the current study, we  
49 therefore used DSI with its much higher angular resolution to offset these problems,  
50 allowing us to examine the relation between high-resolution measurements of white  
51 matter structure and individual differences in metacognitive ability. Based on the  
52 previous findings discussed above, we hypothesized that regional variation of white  
53 matter microstructure would underlie individual differences in metacognitive ability in  
54  
55  
56  
57  
58  
59  
60

each cognitive domain.

## Materials and methods

### *Participants*

Forty-two participants completed the experiment (20 males, age range = 18-47 years, mean age = 21.5 years). Four participants who completed the cognitive testing component were excluded from the brain imaging analysis: one participant because he was left handed, one participant due to suboptimal QA thresholding, and two participants because they had a metal oral appliance that created a large artifact in the DSI scan. Signed informed consent was obtained from all participants prior to completing the study, and ethical approval for the study was obtained from the University of California, Santa Barbara, institutional review board. All participants in the final sample (N = 38) were right handed, had normal or corrected to normal vision and had no history of neurological or psychiatric disease.

### *Stimuli*

Stimuli and tasks were programmed in MATLAB version 7.9 (The Mathworks Inc., Natick, MA, USA) using the Psychophysics Toolbox version 3.0 (Brainard, 1997; Kleiner et al., 2007). Stimuli for the perceptual decision task consisted of visual displays composed of six Gabor gratings arranged in a circle around a fixation point at an eccentricity of 6.5 visual degrees (Figure 1A). Each grating subtended 2.8 visual degrees and consisted of vertical alternating light and dark bars modulated at a spatial frequency of 2.2 cycles per visual degree at a contrast of 20%. Stimuli were presented in a darkened room at a viewing distance of approximately 60cm.

Stimuli for the memory retrieval task consisted of 320 neutral-valence non-composite nouns selected from the Medical Research Council (MRC) Psycholinguistic database (Wilson, 1988). All stimuli were 5 characters in length and had a word frequency between 1 and 800 per million.

### *Tasks and procedure*

Participants performed two experimental sessions: a magnetic resonance imaging (MRI) session in which Diffusion Spectrum Imaging (DSI) scans were acquired and a behavioral session in which they were asked to make metacognitive evaluations of perceptual decisions and mnemonic judgments. A schematic outline of the metacognitive tasks is shown in Figure 1. Task order was counterbalanced across participants.

The perceptual task was adapted from Fleming et al. (2010) and Song et al. (2011). Each trial (N=320) consisted of a presentation of a 250ms visual stimulus display consisting of six Gabor gratings arranged in a circle around central fixation, followed by an interstimulus interval (ISI) of 500ms during which only the fixation cross remained on the screen, followed by a second 250ms stimulus display consisting of six Gabors arranged around fixation (Figure 1A). In one of the two stimulus displays, the orientation of one of the Gabor patches was tilted slightly from the vertical axis. The display interval in which this “pop-out” Gabor occurred as well as its spatial location on the screen varied randomly across trials. The orientation tilt of the pop-out Gabor was adjusted using a 2-

up 1-down adaptive staircase procedure (Fleming et al., 2010; Levitt, 1971) designed to result in a convergence on 70% accuracy for individual performance. Two consecutive correct responses resulted in a reduction of the orientation parameter by one step (0.25 degree), while one incorrect response resulted in an increase of the orientation parameter by one step. Following the offset of the second stimulus presentation, participants made unspeeeded 2-choice discriminations as to whether the pop-out Gabor occurred in either the first or second stimulus display. Participants then rated their confidence in the accuracy of their response on a scale of 1 (low-confidence) to 6 (high-confidence) (Fleming et al., 2010). All responses were made using the number pad on the keyboard.

The memory task consisted of two phases: encoding and recognition. Before beginning the encoding phase, participants were informed that a recognition phase would follow in which their memory for the presented words would be tested. During encoding, participants viewed 160 words randomly selected from the full set of 320 words presented sequentially in the center of the screen. Words were displayed for 1500ms and were separated by an ISI of 1000ms in which a fixation cross was displayed. During recognition, participants were presented with each word from the full list of stimuli in a random order (half of which were presented during encoding and half of which were new), and were asked to make unspeeeded 2-choice discriminations as to whether the stimulus was old or new. Participants then rated their confidence in the accuracy of their response on a scale of 1 (low confidence) to 6 (high confidence). All responses were made using the number pad on the keyboard.

#### *Quantification of metacognitive ability*

Signal detection theory (SDT) (Green & Swets, 1966) was used to compute estimates of metacognitive accuracy, here quantified as the ability of an individual to discriminate between their own correct and incorrect perceptual decisions or mnemonic judgments with confidence ratings on a trial-by-trial basis. A primary concern in any metacognitive (“type II”) analysis is to separate estimates of type II sensitivity from the potential confounding influence of sensitivity on the primary (“type I”) task (e.g., Galvin, Podd, Drga, & Whitmore, 2003). Type II sensitivity refers to an individual’s ability to discriminate between their own correct and incorrect responses, while type I sensitivity refers to an individual’s ability to discriminate between stimulus alternatives (i.e., their capacity to distinguish old items from new items in a recognition memory task) (Clarke, Birdsall, & Tanner, 1959; Higham, Perfect, & Bruno, 2009). SDT approaches can quantify metacognitive accuracy independently of an observer’s decision strategy or cognitive ability on the primary task, which have been shown to confound other methods of estimating metacognitive ability (Fleming & Lau, 2014; Maniscalco & Lau, 2012).

Metacognitive accuracy on the perceptual task was quantified using the computational methods outlined in Fleming et al. (2010). Because performance on the perceptual task is held constant with an online thresholding procedure, it is possible to compute a measure of metacognitive accuracy that is unconfounded by type I performance directly from the empirical type II receiver operating characteristic (ROC) curve. The type II ROC curve reflects the relationship between the accuracy of visual discriminations and an observer’s confidence ratings. To plot the ROC,  $p(\text{confidence}=i \mid \text{correct})$  and  $p(\text{confidence}=i \mid \text{incorrect})$  were calculated for each level of confidence  $i$ , transformed into cumulative probabilities and used to construct each  $x,y$  point on the empirical ROC curve (Fleming



1  
2  
3 et al., 2010; Galvin et al., 2003; Kornbrot, 2006). ROC curves were anchored at [0,0] and  
4 [1,1]. The type II ROC curve thus reflects the probability of being correct for each level  
5 of confidence. An ROC curve that rises steeply off the diagonal axis indicates that the  
6 likelihood of being correct increases with increasing confidence level, while a flat ROC  
7 along the major diagonal indicates a weak relationship between confidence and accuracy.  
8 When several points on the type II ROC are available, an empirical estimate of the area  
9 under the ROC may be obtained, yielding a nonparametric measure of type II sensitivity  
10 (Kornbrot, 2006). The area under the type II ROC curve ( $A_{roc}$ ) when performance is held  
11 constant provides a robust estimate of metacognitive discrimination that is independent of  
12 type I sensitivity. Type I sensitivity ( $d'$ ) was calculated as  $d' = z(H) - z(FA)$ , where  $z$   
13 represents the inverse of the cumulative normal distribution and  $H = p(\text{response}=1 \mid$   
14  $\text{interval}=1)$  and  $FA = p(\text{response}=1 \mid \text{interval}=2)$ .

15  
16  
17  
18 Quantification of metacognitive accuracy in the memory task required a  
19 computational approach that explicitly accounts for type I performance. A model-based  
20 SDT approach to account for variance in primary task performance in the computation of  
21 type II sensitivity has recently been described and validated (Maniscalco & Lau, 2012;  
22 McCurdy et al., 2013). This method has been discussed at length elsewhere (Maniscalco  
23 & Lau, 2012). Briefly, the approach exploits the link between type I and type II SDT  
24 models to express observed type II sensitivity at the level of the type I SDT model  
25 (termed *meta d'*). Maximum likelihood estimation (MLE) is used to determine the  
26 parameter values of the type I SDT model that provide the best fit to the observed type II  
27 data. A measure of metacognitive ability that controls for differences in type I sensitivity  
28 is then calculated by taking the ratio of *meta d'* and the type I sensitivity parameter  $d'$ :  
29  $M_{ratio} = \text{meta } d' / d'$ . The most straightforward approach to computing  $M_{ratio}$  involves an  
30 equal variance SDT model in which the variances of internal distributions of evidence for  
31 categorizing an item as “old” or “new” in the type I model are assumed to be equal.  
32 However, this assumption is violated for 2-choice old/new recognition memory tasks  
33 (Mickes, Wixted, & Wais, 2007; Swets, 1986). We therefore computed  $M_{ratio}$  under an  
34 unequal variance SDT model, which uses the slope of the type I zROC to infer the ratio  
35 of the standard deviations of the type I distributions ( $s$ ) underlying the two response  
36 categories, and then holds this parameter constant in the estimation of  $M_{ratio}$ . Type I  
37 sensitivity ( $d'$ ) was calculated as  $d' = z(H) - z(FA)$ , where  $z$  represents the inverse of the  
38 cumulative normal distribution and  $H = p(\text{response} = \text{old} \mid \text{stimulus} = \text{old})$  and  $FA =$   
39  $p(\text{response} = \text{old} \mid \text{stimulus} = \text{new})$ .

#### 44 45 *MRI acquisition*

46 DSI and T1-weighted anatomical scans were collected on a 3.0 Tesla Siemens Tim  
47 Trio scanner equipped with high-performance gradients at the University of California,  
48 Santa Barbara Brain Imaging Center. DSI scans sampled 257 directions with a maximum  
49 b value of 5000 and an isotropic voxel size of 2.4mm (Axial acquisition, 1 b0 image, TR  
50 = 11.4s, TE = 138ms, 51 slices, FOV = 231×231×123 mm). Before the diffusion-  
51 weighted scan, a high-resolution T1-weighted structural image was acquired using an  
52 MPRAGE pulse sequence (TR = 2300 ms; TE = 2.98 ms; flip angle = 9°; FOV = 256  
53 mm; acquisition voxel size = 1×1×1.1 mm).

#### 56 57 *Diffusion spectrum imaging (DSI) data processing*

58  
59  
60

1  
2  
3  
4  
5  
6  
7  
8  
9  
10  
11  
12  
13  
14  
15  
16  
17  
18  
19  
20  
21  
22  
23  
24  
25  
26  
27  
28  
29  
30  
31  
32  
33  
34  
35  
36  
37  
38  
39  
40  
41  
42  
43  
44  
45  
46  
47  
48  
49  
50  
51  
52  
53  
54  
55  
56  
57  
58  
59  
60

DSI data were reconstructed in DSI Studio ([www.dsi-studio.labsolver.org](http://www.dsi-studio.labsolver.org)) using q-space diffeomorphic reconstruction (QSDR) (Yeh & Tseng, 2011). This technique first nonlinearly spatially normalizes an individual's DSI data and reconstructs spin density functions (SDFs) in standard space. Normalization was performed by registering individual anisotropy maps to the Functional Magnetic Resonance Imaging of the Brain (FMIRB) 1 mm template (FSL, Oxford, UK) using a nonlinear registration implemented in DSI Studio (Ashburner & Friston, 1999). Goodness-of-fit was assessed evaluating the  $R^2$  statistic between the warped image and the template image (Yeh, Tang, & Tseng, 2013). All participants had  $R^2$  above .6, indicating good registration accuracy. QSDR on DSI data are able to reconstruct many complex fiber tract configurations, including crossing fibers. QSDR parameters were mean diffusion distance of 1.25mm and three fiber orientations per voxel.

Deterministic fiber tracking was performed identically to Cieslak & Grafton (2013) using DSI Studio. The parameters included an angular cut-off of  $55^\circ$ , step size of 1.0 mm, minimum length of 10 mm, smoothing of 0.0 mm, maximum length of 400mm and a QA threshold determined by DWI signal in the CSF. Tracking with a modified FACT algorithm was performed until 100,000 streamlines were reconstructed for each individual. Streamlines were labeled according to which the pair of regions in which they terminated. If a streamline did not intersect a labeled voxel within 5mm of its endpoint then the streamline was not considered for analysis.

#### *Structural (T1) data processing*

Cortical surface reconstruction was performed on T1 scans using FreeSurfer (Dale, Fischl, & Sereno, 1999; Fischl & Dale, 2000; Fischl, Liu, & Dale, 2001; Fischl et al., 2002; Fischl, Salat, et al., 2004; Fischl, Sereno, & Dale, 1999; Fischl, Sereno, Tootell, & Dale, 1999; Fischl, van der Kouwe, et al., 2004; Han et al., 2006; Jovicich et al., 2006; Segonne et al., 2004). Affine transformation from b0 space to T1 volume was calculated using Boundary-Based Registration (BBRegister) (Greve & Fischl, 2009). Anatomical scans were segmented using the connectome mapping toolkit (Hagmann et al., 2008). The Lausanne 2008 scale 33 (83 regions) atlas was registered and mapped to the b0 volume from each subject's DSI data. The b0 to MNI voxel mapping produced via QSDR was then used to map region labels from native space to MNI coordinates. Regions were dilated by 4mm in each direction in order to cover the gray/white matter boundary. Dilatation was performed identically to (Cieslak & Grafton, 2013).

#### *White matter microstructure (diffusion anisotropy) data processing*

To examine the relationship between metacognitive ability and white matter microstructure, we computed two high-resolution measures of diffusion anisotropy from DSI scans: generalized fractional anisotropy (GFA) and quantitative anisotropy (QA). These measures extend the fractional anisotropy (FA) measure from diffusion tensor imaging (DTI), which has been used extensively as a measure of white matter microstructure, with changes due to either differences of myelination, axonal density, or degree of fiber crossing (e.g., Kraus et al., 2007; Kubicki et al., 2005). Lower FA values indicate that diffusion is more isotropic (i.e., undirected), whereas higher values indicate that diffusion has a stronger directional orientation. However, as noted above, FA is hindered by the substantial limitations of DTI reconstruction, particularly the partial

1  
2  
3 volume effect (e.g., Barrick & Clark, 2004). Specifically, estimates of FA are influenced  
4 by the presence of crossing fibers and partial volumes of other structures/tissues within a  
5 voxel such as CSF, which can lead to inaccurate measures of anisotropy (Alexander,  
6 Hasan, Lazar, Tsuruda, & Parker, 2001; Oouchi et al., 2007; Vos, Jones, Viergever, &  
7 Leemans, 2011). GFA presents an extension of FA to high-angular resolution diffusion-  
8 weighted images that is capable of measuring anisotropy across multiple diffusion  
9 directions (Tuch, 2004). GFA is computed by dividing the standard deviation by the root  
10 mean square of the SDF. It thus reflects a similar measure of anisotropy to FA but is  
11 generalized across multiple fiber orientations (Cohen-Adad, Descoteaux, & Wald, 2011).  
12 Unfortunately, GFA is also not totally immune from the partial volume effect (Fritzsche,  
13 Laun, Meinzer, & Stieltjes, 2010; Yeh, Verstynen, Wang, Fernández-Miranda, & Tseng,  
14 2013). Quantitative anisotropy (QA), on the other hand, reflects the anisotropy of the  
15 peak orientations of the SDF (Yeh, Wedeen, & Tseng, 2010). QA is calculated by  
16 subtracting the background isotropic diffusion component from the SDF value at the  
17 resolved fiber orientation (Yeh et al., 2010). In the current study, we examined QA for  
18 the peak fiber orientation at each voxel. QA is less susceptible to the partial volume  
19 effect, but it is susceptible to other sources of MR acquisition noise (Yeh et al., 2013b).  
20 Each measure therefore has its relative strengths and both measures present an extension  
21 in high-resolution diffusion-weighted imaging to classical FA measures of white matter  
22 microstructure.  
23

24  
25  
26  
27 GFA and QA values were computed from QSDR reconstructed SDFs in MNI space.  
28 Because our previous investigation (Baird et al., 2013) found right lateralization to neural  
29 structures underlying metacognitive ability, we initially focused our analysis of the  
30 relationship between metacognitive ability and white matter microstructure in the right  
31 hemisphere. To restrict the search volume to white matter (WM), WM masks were  
32 extracted from FreeSurfer parcellation, eroded by 1 voxel, and warped to MNI space  
33 using the diffeomorphic mapping computed from QSDR reconstruction. Masks were then  
34 averaged across subjects and thresholded at .9 to produce an average WM mask. QA and  
35 GFA images were also smoothed with a 4mm full-width at half maximum (FWHM)  
36 Gaussian kernel prior to group-level analysis.  
37  
38  
39

#### 40 *Statistical analysis*

41 Statistical analysis was conducted using the GLM framework implemented in SPM8  
42 (Wellcome Trust Department of Imaging Neuroscience, University College London). For  
43 both QA and GFA, we performed voxelwise multiple regression analyses with  
44 metacognitive accuracy scores and nuisance covariates for age and gender. Cluster-size  
45 tests were used to test for significant regions using a cluster-forming threshold of  $p <$   
46  $0.005$  and a cluster size threshold of  $p < 0.05$  (FWE corrected). Because the assumption  
47 of uniform smoothness (stationarity) is violated for warped structural images, standard  
48 cluster-size tests under random field theory (RFT) are not valid (Hayasaka, Phan,  
49 Liberzon, Worsley, & Nichols, 2004; Worsley, Andermann, Koulis, MacDonald, &  
50 Evans, 1999). We therefore applied a non-stationary cluster extent correction, in which  
51 clusters are adjusted according to local smoothness, using the parametric RFT non-  
52 stationarity correction implemented in the NS toolbox  
53 (<http://fmri.wfubmc.edu/cms/software#NS>). Accounting for non-stationarity is critical as  
54 not performing this correction can lead to invalid conclusions in analysis of structural  
55  
56  
57  
58  
59  
60

1  
2  
3 images (Moorhead et al., 2005). Significant clusters are displayed on FSL's  
4 FMRIB58\_FA\_1mm standard template using MRICro software  
5 (<http://www.cabiatl.com/mricro/mricro/mricro.html>).  
6  
7

## 8 9 Results

### 10 Behavioral results

11  
12 In a counterbalanced design, participants (N=42) completed a perceptual  
13 discrimination task and verbal recognition memory task in which they made 2-choice  
14 discriminations and then rated their confidence in the accuracy of their responses on a  
15 trial-by-trial basis (Figure 1) (Fleming et al., 2010; McCurdy et al., 2013). The perceptual  
16 task was performed at an individually determined threshold using a 2-up 1-down adaptive  
17 staircase procedure that results in a convergence on 70% accuracy at the limit for  
18 individual performance (Fleming et al., 2010; Levitt, 1971). Analysis revealed that  
19 performance accuracy was well controlled by the staircase for all participants ( $M = 0.707$ ,  
20  $SD = 0.02$ ,  $range = 0.67-0.73$ ). Overall, performance on the memory task was good and  
21 had similar mean accuracy ( $M = 0.69$ ,  $SD = 0.08$ ,  $range = 0.58-0.93$ ).  
22  
23

24  
25 A linear mixed model with participant included as a random effect revealed that RT  
26 significantly predicted confidence at the trial level in both the perceptual decision task ( $t$   
27  $= -34.75$ ,  $p < .001$ ;  $int = 3.76$ ,  $estimate = -0.40$ ) and memory retrieval task ( $t = -28.45$ ,  $p <$   
28  $.001$ ;  $int = 4.39$ ,  $estimate = -0.17$ ), indicating that more confident decisions were  
29 associated with faster responses. Overall, mean confidence was higher in the memory  
30 retrieval task ( $M = 4.01$ ,  $SD = 0.59$ ) compared to the perceptual decision task ( $M = 3.27$ ,  
31  $SD = 0.96$ ) [ $t(41) = 5.32$ ,  $p < .001$ ], which may be attributed to the relative difficulty of  
32 the perceptual task which was performed at an individually determined perceptual  
33 threshold. Mean confidence level also showed a significant correlation within individuals  
34 across the two tasks ( $r(42) = 0.41$ ,  $p < .01$ ). Together these results replicate previous  
35 findings (Baird et al., 2013; Fleming et al., 2012; Song et al., 2011) and suggest that  
36 confidence level reflects both a task-independent general level of confidence particular to  
37 an individual as well as a task-dependent level of confidence an individual has toward  
38 performance on a particular cognitive task.  
39  
40

41  
42 Signal detection theory (SDT) (Green & Swets, 1966) was used to quantify individual  
43 differences in metacognitive ability ("type II sensitivity"); here quantified as the ability to  
44 accurately link confidence with performance (see *Quantification of metacognitive*  
45 *ability*). SDT enables computational approaches to the quantification of type II sensitivity  
46 that is independent of the potential confounding influence of type I sensitivity ( $d'$ ) on the  
47 primary task. Analysis confirmed that metacognitive ability in both the perceptual  
48 decision task ( $A_{roc}$ ) and recognition memory task ( $M_{ratio}$ ) were uncorrelated with type I  
49 performance ( $A_{roc}$ :  $r(40) = 0.07$ ,  $p = 0.67$ ;  $M_{ratio}$ :  $r(40) = -0.29$ ,  $p = 0.06$ ). Additionally,  
50 orientation discrimination threshold in the perceptual task was uncorrelated with  
51 perceptual  $A_{roc}$  ( $r(40) = -0.11$ ,  $p = 0.49$ ), indicating that  $A_{roc}$  estimates were not  
52 confounded with variance in perceptual acuity. SDT estimates of metacognitive ability  
53 were thus confirmed to be independent of variance in primary task performance, allowing  
54 for a direct comparison of metacognitive ability across process domains. Analysis  
55 revealed that metacognitive accuracy for perceptual decisions ( $A_{roc}$ ) and mnemonic  
56  
57  
58  
59  
60

1  
2  
3 judgments ( $M_{\text{ratio}}$ ) were uncorrelated across individuals ( $r(40) = 0.15, p = 0.34$ ),  
4 indicating an intra-individual dissociation in metacognitive ability across process  
5 domains (Figure 2). To ensure that this result was not an artifact of the fact that  
6 metacognitive ability for memory and perception were in different units ( $M_{\text{ratio}}$  and  $A_{\text{roc}}$ ),  
7 we calculated  $M_{\text{ratio}}$  for the perceptual discrimination task and correlated it with  $M_{\text{ratio}}$  for  
8 the memory task. These measures were also uncorrelated across individuals ( $r(40) = -$   
9  $0.07, p = 0.64$ ), indicating that the lack of correlation between perceptual and mnemonic  
10 metacognitive ability in our data cannot be attributed to differences in the computational  
11 approach or numerical scale between  $M_{\text{ratio}}$  and  $A_{\text{roc}}$ . This result replicates two recent  
12 experiments using identical tasks and behavioral experimental designs (Baird et al., 2013;  
13 Baird, Mrazek, Phillips, & Schooler, 2014). However, given that this finding is a null  
14 result, it nevertheless must be interpreted cautiously given the limited statistical power of  
15 each individual experiment. To increase the statistical power of this test, we therefore  
16 aggregated the data across these multiple studies to create a pooled sample of 135  
17 participants. Integrated data analysis of this aggregated sample also revealed no  
18 correlation between metacognitive ability across memory and perception tasks ( $r(133) =$   
19  $0.05, p = 0.57$ ).  
20  
21  
22  
23

#### 24 *White matter microstructure and tractography results*

25 We next evaluated the relationship between white matter microstructure (diffusion  
26 anisotropy) and metacognitive ability for memory and perception. As shown in Figure 3A  
27 and Table 1, metacognitive accuracy for perceptual decisions ( $A_{\text{roc}}$ ) was associated with  
28 significantly increased generalized fractional anisotropy in the white matter underlying  
29 the right anterior cingulate cortex (ACC) ( $p < .05$ , FWec; voxelwise threshold  $p < .005$ ).  
30 No suprathreshold clusters were observed between  $A_{\text{roc}}$  and quantitative anisotropy. As  
31 shown in Figure 3B and Table 1, metacognitive accuracy for memory retrieval ( $M_{\text{ratio}}$ )  
32 was associated with increased quantitative anisotropy in the white matter extending into  
33 the inferior parietal lobule (IPL) in the region of the angular gyrus ( $p < .05$ , FWec;  
34 voxelwise threshold  $p < .005$ ). No suprathreshold clusters were observed between  $M_{\text{ratio}}$   
35 and generalized fractional anisotropy. Additionally, no significant regions were observed  
36 linking variation in white matter microstructure in the left hemisphere to either  
37 metacognitive variable, and no significant regions were observed in which white matter  
38 microstructure negatively correlated with metacognitive ability in either domain.  
39  
40  
41  
42

43 We followed up this analysis by examining the anatomical connections of IPL and  
44 ACC white matter regions. For each cluster, we collected all streamlines that passed  
45 through the cluster, grouping the tracts according to the cortical regions they connected  
46 (see *Diffusion spectrum imaging (DSI) data processing*). We considered pairs of regions  
47 to be connected through the cluster if greater than 70% of the sample had streamlines  
48 connecting these regions passing through the cluster. As shown in Figure 4a, results  
49 revealed that the ACC white matter cluster connected 3 pairs of regions: right anterior  
50 superior frontal gyrus (aSFG) to the right caudal ACC, right aSFG to left aSFG, and right  
51 aSFG to left caudal ACC. As shown in Figure 4b, the IPL white matter cluster connected  
52 10 pairs of regions: right IPL to right caudal middle frontal gyrus (MFG), right IPL to  
53 right precentral gyrus, right IPL to right postcentral gyrus, a within-area right IPL  
54 connection to right supramarginal gyrus, right IPL to right inferior temporal gyrus, right  
55 IPL to middle temporal gyrus, right IPL to the banks of the superior temporal sulcus,  
56  
57  
58  
59  
60

1  
2  
3 right precentral gyrus to right inferior temporal gyrus, right precentral gyrus to right  
4 middle temporal gyrus, and right supramarginal gyrus to right middle temporal gyrus.  
5  
6

## 7 8 **Discussion** 9

10  
11 Replicating our previous studies (Baird et al., 2013; Baird et al., 2014), we found that  
12 the capacity of an individual to make accurate metacognitive evaluations of perceptual  
13 decisions and memory were uncorrelated, indicating an intra-individual dissociation in  
14 metacognitive ability across domains. This finding bolsters previous evidence for the  
15 notion that metacognitive skill in one domain may not necessarily translate to another  
16 (David et al., 2012; Pannu & Kaszniak, 2005; Schnyer et al., 2004; Metcalfe et al., 2012).  
17 Furthermore, our results indicate that metacognitive accuracy in each domain was related  
18 to regional differences of white matter microstructure. Metacognitive ability in the  
19 perceptual domain was associated with increased generalized fractional anisotropy in the  
20 white matter underlying the right anterior cingulate cortex (ACC), whereas metacognitive  
21 ability in the memory domain was associated with increased quantitative anisotropy in  
22 the white matter extending into the right inferior parietal lobule (IPL)<sup>1</sup>. Together, these  
23 results extend previous findings linking metacognitive ability in the domains of  
24 perception and memory to differences in distinct gray matter volume (McCurdy et al.,  
25 2013) and resting-state functional connectivity (Baird et al., 2013).  
26  
27

28 Tractography analysis of the right ACC white matter cluster associated with increased  
29 metacognitive ability on the perceptual task revealed that this region connected right  
30 aPFC (specifically the anterior superior frontal gyrus) to the right caudal ACC, right  
31 aPFC to left aPFC, and right aPFC to left caudal ACC. These results overlap with a  
32 recent connectivity-based parcellation of the human cingulate cortex, which revealed that  
33 this region has prominent anatomical connections to lateral aPFC, as well as the dorsal  
34 striatum (caudate nucleus and putamen) (Beckmann, Johansen-Berg, & Rushworth,  
35 2009). The finding that metacognitive ability on the perceptual discrimination task was  
36 linked to increased white matter anisotropy underlying the ACC therefore provides  
37 convergent evidence with our recent finding that metacognitive accuracy in this same  
38 task is associated with increased resting-state functional connectivity between lateral  
39 aPFC and the dorsal anterior cingulate cortex (dACC) and dorsal striatum (Baird et al.,  
40 2013). This finding also converges with other work linking metacognitive ability in the  
41 perceptual domain to the anatomically adjacent dACC, particularly the observation that  
42 lateral aPFC and dACC show increased activation during metacognitive assessments of  
43 visual discriminations and that the strength of activation in these regions during  
44 metacognitive judgments correlates with reported confidence (Fleming et al., 2012). A  
45 previous DTI study also found a positive association between perceptual metacognitive  
46 ability and fractional anisotropy in the anterior callosum linking left and right aPFC  
47 (Fleming et al., 2010). While we did not observe a direct relationship between  
48 metacognitive ability and diffusion anisotropy in the anterior callosum, our tractography  
49 analysis revealed that the significant white matter cluster observed in our study contains  
50 fibers that pass through the anterior callosum connecting left and right aPFC, consistent  
51 with this previous result.  
52  
53  
54  
55  
56  
57  
58  
59  
60

1  
2  
3  
4  
5  
6  
7  
8  
9  
10  
11  
12  
13  
14  
15  
16  
17  
18  
19  
20  
21  
22  
23  
24  
25  
26  
27  
28  
29  
30  
31  
32  
33  
34  
35  
36  
37  
38  
39  
40  
41  
42  
43  
44  
45  
46  
47  
48  
49  
50  
51  
52  
53  
54  
55  
56  
57  
58  
59  
60

In the memory domain, we found that the ability to make accurate metacognitive judgments was associated with increased diffusion anisotropy in tracts extending into right IPL in the region near the angular gyrus. This finding is consistent with a broad range of studies documenting a primary role of IPL in meta-memory (e.g., Chua, Schacter, Rand-Giovannetti, & Sperling, 2006; Chua, Schacter, & Sperling, 2009; Elman, Klostermann, Marian, Verstaen, & Shimamura, 2012). For instance, greater activity in a network including anterior prefrontal, mid/posterior cingulate, and lateral parietal regions is observed during memory monitoring in both feeling-of-knowing and retrospective confidence tasks (e.g., Chua et al., 2006; Chua et al., 2009). Moreover, IPL also shows greater activation for high confidence hits in meta-memory tasks (Kim & Cabeza, 2007; Wheeler & Buckner, 2004) as well as strong “feeling-of-knowing” judgments for semantic and episodic information (Elman et al., 2012). Finally, patients with parietal lesions produce fewer high confidence recognition responses during retrieval (Davidson et al., 2008; Simons, Peers, Mazuz, Berryhill, & Olson, 2010). This finding is also consistent with our recent observation that metacognitive ability for memory is associated with increased functional connectivity in a network including medial aPFC, middle frontal gyrus (MFG) and IPL (Baird et al., 2013). Tractography analysis of the significant IPL white matter cluster revealed that it contained prominent anatomical tracts connecting inferior parietal regions to the MFG, temporal lobe and precentral gyrus, indicating a partial overlap in anatomical and functional networks underlying mnemonic metacognitive skill.

Altogether, the current findings converge with previous results in support of the proposal that an individual’s capacity to accurately reflect on their cognitive processes is at least partially dependent on the type of cognitive process they are reflecting upon. Within this context, one possibility is that metacognitive evaluations in perceptual discrimination tasks primarily involve the capacity to monitor active representations. This type of metacognition may be best conceived of as an online monitor that integrates information over short timescales, and may be linked to the related construct of cognitive control (Fernandez-Duque, Baird, & Posner, 2000; Fleming & Dolan, 2012). Indeed, white matter microstructure in the region of the anterior cingulate has also been linked to cognitive control (Metzler-Baddeley et al., 2012), and meta-analysis of functional imaging studies indicates that the anatomically adjacent dACC supports key control functions such as conflict and error detection (Beckmann et al., 2009) (see Ridderinkhof, Ullsperger, Crone, & Nieuwenhuis, 2004 for a review). If metacognitive ability in perceptual discrimination tasks involves the accessibility of performance monitoring information in dACC to a wider network (Baird et al., 2013; Fleming et al., 2012), then microstructure in this region should play a key role. The current results are therefore consistent with a hypothesis put forward by Fleming et al. (2012) and Fleming & Dolan (2012) that metacognitive assessment of perceptual discriminations depend on the accessibility of information pertaining to the monitoring of immediate decisions (including errors and conflict, encoded in regions such as the dACC) to aPFC, which governs the transfer that information to a global frame of reference for metacognitive report.

In contrast, accurate metacognitive evaluations of memory may be understood to involve an appraisal of information pertaining to the content of memory, such as assessing the strength of a memory trace (Nelson & Narens, 1990). As noted above,

1  
2  
3 functional imaging studies of recognition memory and meta-memory frequently observe  
4 activation in IPL alongside activation in the medial temporal lobe across a wide array of  
5 stimuli and test conditions (e.g., Chua et al., 2006; Chua et al., 2009; Elman et al., 2012;  
6 Kim & Cabeza, 2007; Wheeler & Buckner, 2004). While specifying the precise function  
7 of this region is a topic of active research, at least four different theories all implicate IPL  
8 in some form of coding of information pertaining to memory or in directing attention to  
9 memory representations (for review see Cabeza, Ciaramelli, Olson, & Moscovitch, 2008;  
10 Olson & Berryhill, 2009; Wagner, Shannon, Kahn, & Buckner, 2005). For instance, IPL  
11 has been proposed to serve as an accumulator for the strength of evidence for or against a  
12 memory decision (Wagner et al., 2005), to dynamically represent retrieved information as  
13 an output buffer (Baddeley, 2000; Vilberg & Rugg, 2008; Vilberg, Moosavi, & Rugg,  
14 2006), or to support the subjective experience of the vividness of memories (Ally,  
15 Simons, McKeever, Peers, & Budson, 2008). Accordingly, the finding that increased  
16 anisotropy in the white matter extending into IPL underlies enhanced metacognitive  
17 ability for memory may reflect the accessibility of memory information in IPL in the  
18 form of buffered episodic information, a memory strength signal, or memory vividness.  
19 Further elucidating the functional significance of this finding will be an important topic  
20 for future research.

21  
22 As noted above, the finding that metacognitive ability across mnemonic and  
23 perceptual tasks did not correlate across individuals replicates two recent experiments  
24 using identical tasks and behavioral experimental designs (Baird et al., 2013; Baird,  
25 Mrazek, Phillips, & Schooler, 2014). Furthermore, integrative data analysis of these  
26 studies combined with the current data indicates that the aggregated sample of  
27 participants from these studies (N=135) also revealed no correlation between  
28 metacognitive ability across domains. While we think that these results are clear and  
29 convincing, we nevertheless note that drawing firm conclusions regarding the behavioral  
30 stability of metacognitive accuracy across cognitive domains at the present time would  
31 still be premature. Aside from the current results and the two studies noted above, which  
32 all used identical tasks, only one other study (McCurdy et al., 2013) has compared  
33 metacognitive ability for perceptual and mnemonic judgments within individuals. As  
34 discussed above, the voxel-based morphometry findings of McCurdy et al. converge with  
35 Baird et al. (2013) and the current study in suggesting that individual differences in  
36 metacognitive ability for perception and memory relate to distinct features of brain  
37 architecture, and offer mutual support for some of the primary candidate brain regions.  
38 However, despite the dissociation at the neural level, McCurdy et al. reported a positive  
39 correlation between behavioral scores for perceptual and mnemonic metacognitive ability.  
40 One possibility is that this discrepancy could be attributed to differences between the  
41 tasks. For example, the memory task used in the current experiments involved a longer  
42 retention interval than the task used in McCurdy et al. Additionally, the memory task  
43 used in McCurdy et al. was a 2-alternative forced choice (2AFC) task whereas our  
44 experiments have employed a 2-choice old/new discrimination task, and there are  
45 differences between these two types of memory tests in the recruitment of recollection  
46 (Cook, Marsh, & Hicks, 2005). Therefore, whereas McCurdy et al. employed a 2AFC  
47 design for both tasks, the current study used a 2AFC task for the perceptual task and a 2-  
48 choice old/new discrimination task for the memory task. Whether or how this difference  
49 in task structure across cognitive domains impacts individual performance, and thus the  
50  
51  
52  
53  
54  
55  
56  
57  
58  
59  
60



1  
2  
3 stability of metacognitive accuracy across domains, remains unclear. It will therefore be  
4 important for future research to examine the effect of manipulating the type and  
5 uncertainty of the type I discrimination to observe whether there are some circumstances  
6 that are more conducive to observing a generalized metacognitive ability.  
7

8 Additionally, although the present findings and those of Baird et al. (2013) and  
9 McCurdy et al. (2013) call into question a strict homogeneity of metacognition at the  
10 neural level, it is important to bear in mind that the individual differences approach used  
11 in these studies identifies differences that underlie the capacity for accurate  
12 metacognitive assessment rather than a comprehensive account of the neural processes  
13 that contribute to metacognitive judgments. The regional specificity observed in white  
14 matter microstructure, gray matter volume and functional connectivity identified across  
15 these studies should therefore primarily be regarded to reflect cross-sectional differences  
16 that underlie the capacity for accurate metacognition, rather than an exhaustive account  
17 of the neural processes that contribute to metacognitive judgments in either domain.  
18 Indeed, it remains plausible that some domain-general regions may be recruited across  
19 different types of metacognitive tasks, a possibility that is supported by task-based  
20 comparisons of confidence judgments in memory and perception tasks using fMRI (Fleck,  
21 Daselaar, Dobbins, & Cabeza, 2006).  
22

23  
24 In conclusion, the current findings demonstrate that the ability to make accurate  
25 metacognitive evaluations in perceptual and mnemonic domains relate to regional  
26 differences of white matter microstructure, and lend support to the recent finding that  
27 metacognitive ability in each of these domains is linked to the strength of functional  
28 coupling within distinct cortical networks (Baird et al., 2013). These findings also  
29 illustrate how the investigation of white matter structure with high-resolution diffusion  
30 spectrum imaging can capture anatomical variation in white matter connection strengths  
31 (which may be inaccessible to other techniques) that are important to higher-order  
32 cognitive functions.  
33  
34  
35  
36  
37

### 38 Notes

39 1. The finding that metacognitive ability on each task was related differentially to QA  
40 and GFA is not fully understood, and this differential effect was unexpected. At the  
41 current time there is insufficient knowledge about the underlying tissue structure to  
42 predict when they will provide the same or different results. At this point, they are  
43 complementary techniques. Furthermore, given that GFA and QA are susceptible to  
44 different sources of MR noise (i.e., receiver gain or B1 inhomogeneity), we cannot rule  
45 out that the differential effect on GFA and QA may be related to differences in the  
46 sensitivity of these measures across different brain regions (Yeh et al., 2013b).  
47  
48  
49  
50  
51  
52  
53  
54  
55  
56  
57  
58  
59  
60

## Acknowledgments

We thank Philip Beach, Mario Mendoza, Michael Mrazek and Benjamin Mooneyham for assistance in conducting the research. We acknowledge support from the Center for Scientific Computing at the CNSI and MRL: an NSF MRSEC (DMR-1121053) and NSF CNS-0960316. B. B. was supported by a National Science Foundation Graduate Research Fellowship under Grant No. DGE-0707430. This research was supported by a grant from the U.S. Department of Education Grant R305A110277 awarded to J. W. S. The content of this article does not necessarily reflect the position or policy of the U.S. Government, and no official endorsement should be inferred.

For Review Only

1  
2  
3  
4  
5  
6  
7  
8  
9  
10  
11  
12  
13  
14  
15  
16  
17  
18  
19  
20  
21  
22  
23  
24  
25  
26  
27  
28  
29  
30  
31  
32  
33  
34  
35  
36  
37  
38  
39  
40  
41  
42  
43  
44  
45  
46  
47  
48  
49  
50  
51  
52  
53  
54  
55  
56  
57  
58  
59  
60

## References

- Alexander, A. L., Hasan, K. M., Lazar, M., Tsuruda, J. S., & Parker, D. L. (2001). Analysis of partial volume effects in diffusion tensor MRI. *Magnetic Resonance in Medicine*, 45(5), 770-780.
- Ally, B. A., Simons, J. S., McKeever, J. D., Peers, P. V., & Budson, A. E. (2008). Parietal contributions to recollection: electrophysiological evidence from aging and patients with parietal lesions. *Neuropsychologia*, 46(7), 1800-1812.
- Andrews-Hanna, J. R., Reidler, J. S., Sepulcre, J., Poulin, R., & Buckner, R. L. (2010). Functional-anatomic fractionation of the brain's default network. *Neuron*, 65(4), 550-562.
- Ashburner, J., & Friston, K. J. (1999). Nonlinear spatial normalization using basis functions. *Human brain mapping*, 7(4), 254-266.
- Baddeley, A. (2000). The episodic buffer: a new component of working memory? *Trends Cogn Sci*, 4(11), 417-423.
- Baird, B., Smallwood, J., Gorgolewski, K. J., & Margulies, D. S. (2013). Medial and Lateral Networks in Anterior Prefrontal Cortex Support Metacognitive Ability for Memory and Perception. *The Journal of Neuroscience*, 33(42), 16657-16665.
- Baird, B., Mrazek, M., Phillips, D. T., & Schooler, J. W. (2014). Domain-specific enhancement of metacognitive ability following meditation training. *Journal of Experimental Psychology: General*.
- Barrick, T. R., & Clark, C. A. (2004). Singularities in diffusion tensor fields and their relevance in white matter fiber tractography. *Neuroimage*, 22(2), 481-491.
- Beckmann, M., Johansen-Berg, H., & Rushworth, M. F. (2009). Connectivity-based parcellation of human cingulate cortex and its relation to functional specialization. *The Journal of Neuroscience*, 29(4), 1175-1190.
- Brainard, D. H. (1997). The Psychophysics Toolbox. *Spat Vis*, 10(4), 433-436.
- Buckner, R. L., Andrews-Hanna, J. R., & Schacter, D. L. (2008). The brain's default network: anatomy, function, and relevance to disease. *Ann N Y Acad Sci*, 1124, 1-38.
- Cabeza, R., Ciaramelli, E., Olson, I. R., & Moscovitch, M. (2008). The parietal cortex and episodic memory: an attentional account. *Nature Reviews Neuroscience*, 9(8), 613-625.
- Christoff, K., Gordon, A. M., Smallwood, J., Smith, R., & Schooler, J. W. (2009). Experience sampling during fMRI reveals default network and executive system contributions to mind wandering. *Proc Natl Acad Sci*, 106(21), 8719-8724.
- Chua, E. F., Schacter, D. L., Rand-Giovannetti, E., & Sperling, R. A. (2006). Understanding metamemory: Neural correlates of the cognitive process and subjective level of confidence in recognition memory. *NeuroImage*, 29, 1150-1160.
- Chua, E. F., Schacter, D. L., & Sperling, R. A. (2009). Neural correlates of metamemory: a comparison of feeling-of-knowing and retrospective confidence judgments. *J Cogn Neurosci*, 21(9), 1751-1765.
- Cieslak, M., & Grafton, S. T. (2014). Local termination pattern analysis: a tool for comparing white matter morphology. *Brain imaging and behavior*, 8(2), 292-299.

- 1  
2  
3  
4  
5  
6  
7  
8  
9  
10  
11  
12  
13  
14  
15  
16  
17  
18  
19  
20  
21  
22  
23  
24  
25  
26  
27  
28  
29  
30  
31  
32  
33  
34  
35  
36  
37  
38  
39  
40  
41  
42  
43  
44  
45  
46  
47  
48  
49  
50  
51  
52  
53  
54  
55  
56  
57  
58  
59  
60
- Clarke, F. R., Birdsall, T. G., & Tanner, W. (1959). Two types of ROC curves and definitions of parameters. *The Journal of the Acoustical Society of America*, *31*(5), 629-630.
- Cohen-Adad, J., Descoteaux, M., & Wald, L. L. (2011). Quality assessment of high angular resolution diffusion imaging data using bootstrap on Q-ball reconstruction. *Journal of Magnetic Resonance Imaging*, *33*(5), 1194-1208.
- Dale, A. M., Fischl, B., & Sereno, M. I. (1999). Cortical surface-based analysis. I. Segmentation and surface reconstruction. *Neuroimage*, *9*(2), 179-194.
- David, A. S., Bedford, N., Wiffen, B., & Gilleen, J. (2012). Failures of metacognition and lack of insight in neuropsychiatric disorders. *Philosophical Transactions of the Royal Society B: Biological Sciences*, *367*(1594), 1379-1390.
- Davidson, P. S. R., Anaki, D., Ciaramelli, E., Cohn, M., Kim, A. S. N., Murphy, K. J., et al. (2008). Does lateral parietal cortex support episodic memory?: Evidence from focal lesion patients. *Neuropsychologia*, *46*(7), 1743-1755.
- Elman, J. A., Klostermann, E. C., Marian, D. E., Verstaen, A., & Shimamura, A. P. (2012). Neural correlates of metacognitive monitoring during episodic and semantic retrieval. *Cogn Affect Behav Neurosci*, *12*(3), 599-609.
- Fernandez-Duque, D., Baird, J. A., & Posner, M. I. (2000). Executive attention and metacognitive regulation. *Conscious Cogn*, *9*(2 Pt 1), 288-307.
- Fischl, B., & Dale, A. M. (2000). Measuring the thickness of the human cerebral cortex from magnetic resonance images. *Proc Natl Acad Sci U S A*, *97*(20), 11050-11055.
- Fischl, B., Liu, A., & Dale, A. M. (2001). Automated manifold surgery: constructing geometrically accurate and topologically correct models of the human cerebral cortex. *IEEE Trans Med Imaging*, *20*(1), 70-80.
- Fischl, B., Salat, D. H., Busa, E., Albert, M., Dieterich, M., Haselgrove, C., et al. (2002). Whole brain segmentation: automated labeling of neuroanatomical structures in the human brain. *Neuron*, *33*(3), 341-355.
- Fischl, B., Salat, D. H., van der Kouwe, A. J., Makris, N., Segonne, F., Quinn, B. T., et al. (2004). Sequence-independent segmentation of magnetic resonance images. *Neuroimage*, *23 Suppl 1*, S69-84.
- Fischl, B., Sereno, M. I., & Dale, A. M. (1999). Cortical surface-based analysis. II: Inflation, flattening, and a surface-based coordinate system. *Neuroimage*, *9*(2), 195-207.
- Fischl, B., Sereno, M. I., Tootell, R. B., & Dale, A. M. (1999). High-resolution intersubject averaging and a coordinate system for the cortical surface. *Hum Brain Mapp*, *8*(4), 272-284.
- Fischl, B., van der Kouwe, A., Destrieux, C., Halgren, E., Segonne, F., Salat, D. H., et al. (2004). Automatically parcellating the human cerebral cortex. *Cereb Cortex*, *14*(1), 11-22.
- Fleck, M. S., Daselaar, S. M., Dobbins, I. G., & Cabeza, R. (2006). Role of prefrontal and anterior cingulate regions in decision-making processes shared by memory and nonmemory tasks. *Cereb Cortex*, *16*(11), 1623-1630.
- Fleming, S. M., & Dolan, R. J. (2012). The neural basis of metacognitive ability. *Philos Trans R Soc Lond B Biol Sci*, *367*(1594), 1338-1349.

- 1  
2  
3 Fleming, S. M., Dolan, R. J., & Frith, C. D. (2012). Metacognition: computation, biology  
4 and function. *Philosophical Transactions of the Royal Society B: Biological*  
5 *Sciences*, 367(1594), 1280-1286.
- 6  
7 Fleming, S. M., Huijgen, J., & Dolan, R. J. (2012). Prefrontal contributions to  
8 metacognition in perceptual decision making. *J Neurosci*, 32(18), 6117-6125.
- 9  
10 Fleming, S. M., & Lau, H. C. (2014). How to measure metacognition. *Name: Frontiers in*  
11 *Human Neuroscience*, 8, 443.
- 12  
13 Fleming, S. M., Weil, R. S., Nagy, Z., Dolan, R. J., & Rees, G. (2010). Relating  
14 introspective accuracy to individual differences in brain structure. *Science*,  
15 329(5998), 1541-1543.
- 16  
17 Fritzsche, K. H., Laun, F. B., Meinzer, H.-P., & Stieltjes, B. (2010). Opportunities and  
18 pitfalls in the quantification of fiber integrity: What can we gain from Q-ball  
19 imaging? *Neuroimage*, 51(1), 242-251.
- 20  
21 Galvin, S. J., Podd, J. V., Drga, V., & Whitmore, J. (2003). Type 2 tasks in the theory of  
22 signal detectability: discrimination between correct and incorrect decisions.  
23 *Psychon Bull Rev*, 10(4), 843-876.
- 24  
25 Gazzaniga, M. S., & LeDoux, J. E. (1978). *The Integrated Mind*. New York: Plenum  
26 Press.
- 27  
28 Green, D. M., & Swets, J. A. (1966). *Signal detection theory and psychophysics*: Wiley.
- 29  
30 Greve, D. N., & Fischl, B. (2009). Accurate and robust brain image alignment using  
31 boundary-based registration. *Neuroimage*, 48(1), 63.
- 32  
33 Hall, L., Johansson, P., Tärning, B., Sikström, S., & Deutgen, T. (2010). Magic at the  
34 marketplace: Choice blindness for the taste of jam and the smell of tea. *Cognition*,  
35 117(1), 54-61.
- 36  
37 Hagemann, P., Cammoun, L., Gigandet, X., Meuli, R., Honey, C. J., Wedeen, V. J., &  
38 Sporns, O. (2008). Mapping the structural core of human cerebral cortex. *PLoS*  
39 *biology*, 6(7), e159.
- 40  
41 Han, X., Jovicich, J., Salat, D., van der Kouwe, A., Quinn, B., Czanner, S., et al. (2006).  
42 Reliability of MRI-derived measurements of human cerebral cortical thickness:  
43 the effects of field strength, scanner upgrade and manufacturer. *Neuroimage*,  
44 32(1), 180-194.
- 45  
46 Hayasaka, S., Phan, K. L., Liberzon, I., Worsley, K. J., & Nichols, T. E. (2004).  
47 Nonstationary cluster-size inference with random field and permutation methods.  
48 *Neuroimage*, 22(2), 676-687.
- 49  
50 Higham, P. A., Perfect, T. J., & Bruno, D. (2009). Investigating strength and frequency  
51 effects in recognition memory using type-2 signal detection theory. *Journal of*  
52 *Experimental Psychology: Learning, Memory, and Cognition*, 35(1), 57.
- 53  
54 Johansson, P., Hall, L., Sikström, S., & Olsson, A. (2005). Failure to detect mismatches  
55 between intention and outcome in a simple decision task. *Science*, 310(5745),  
56 116-119.
- 57  
58 Jones, D.K., Knösche, T.R. & Turner, R. (2013). White matter integrity, fiber count, and  
59 other fallacies: The do's and don'ts of diffusion MRI. *NeuroImage*, 73, 239-254.
- 60  
61 Jovicich, J., Czanner, S., Greve, D., Haley, E., van der Kouwe, A., Gollub, R., et al.  
(2006). Reliability in multi-site structural MRI studies: effects of gradient non-  
linearity correction on phantom and human data. *Neuroimage*, 30(2), 436-443.

- 1  
2  
3 Kim, H., & Cabeza, R. (2007). Trusting our memories: dissociating the neural correlates  
4 of confidence in veridical versus illusory memories. *The Journal of Neuroscience*,  
5 27(45), 12190-12197.  
6  
7 Kleiner, M., Brainard, D., Pelli, D., Ingling, A., Murray, R., & Broussard, C. (2007).  
8 What's new in Psychtoolbox-3. *Perception*, 36(14), 1.1-16.  
9  
10 Kornbrot, D. E. (2006). Signal detection theory, the approach of choice: model-based and  
11 distribution-free measures and evaluation. *Percept Psychophys*, 68(3), 393-414.  
12  
13 Kraus, M. F., Susmaras, T., Caughlin, B. P., Walker, C. J., Sweeney, J. A., & Little, D. M.  
14 (2007). White matter integrity and cognition in chronic traumatic brain injury: a  
15 diffusion tensor imaging study. *Brain*, 130(10), 2508-2519.  
16  
17 Kubicki, M., Park, H., Westin, C., Nestor, P., Mulkern, R., Maier, S., et al. (2005). DTI  
18 and MTR abnormalities in schizophrenia: analysis of white matter integrity.  
19 *Neuroimage*, 26(4), 1109-1118.  
20  
21 Levitt, H. (1971). Transformed up-down methods in psychoacoustics. *The Journal of the*  
22 *Acoustical society of America*, 49, 2-467.  
23  
24 Makris, N., Kennedy, D. N., McInerney, S., Sorensen, A. G., Wang, R., Caviness, V. S.,  
25 et al. (2005). Segmentation of subcomponents within the superior longitudinal  
26 fascicle in humans: a quantitative, in vivo, DT-MRI study. *Cerebral Cortex*, 15(6),  
27 854-869.  
28  
29 Maniscalco, B., & Lau, H. (2012). A signal detection theoretic approach for estimating  
30 metacognitive sensitivity from confidence ratings. *Conscious Cogn*, 21(1), 422-  
31 430.  
32  
33 McCaig, R. G., Dixon, M., Keramatian, K., Liu, I., & Christoff, K. (2011). Improved  
34 modulation of rostral lateral prefrontal cortex using real-time fMRI training and  
35 meta-cognitive awareness. *Neuroimage*, 55(3), 1298-1305.  
36  
37 McCurdy, L. Y., Maniscalco, B., Metcalfe, J., Liu, K. Y., de Lange, F. P., & Lau, H.  
38 (2013). Anatomical Coupling between Distinct Metacognitive Systems for  
39 Memory and Visual Perception. *The Journal of Neuroscience*, 33(5), 1897-1906.  
40  
41 Metcalfe, J. E., & Shimamura, A. P. (1994). *Metacognition: Knowing about knowing*:  
42 The MIT Press.  
43  
44 Metcalfe, J., Van Snellenberg, J. X., DeRosse, P., Balsam, P., & Malhotra, A. K. (2012).  
45 Judgements of agency in schizophrenia: an impairment in auto-noetic  
46 metacognition. *Philosophical Transactions of the Royal Society B: Biological*  
47 *Sciences*, 367(1594), 1391-1400.  
48  
49 Metzler-Baddeley, C., Jones, D. K., Steventon, J., Westacott, L., Aggleton, J. P., &  
50 O'Sullivan, M. J. (2012). Cingulum microstructure predicts cognitive control in  
51 older age and mild cognitive impairment. *The Journal of Neuroscience*, 32(49),  
52 17612-17619.  
53  
54 Mickes, L., Wixted, J. T., & Wais, P. E. (2007). A direct test of the unequal-variance  
55 signal detection model of recognition memory. *Psychon Bull Rev*, 14(5), 858-865.  
56  
57 Moorhead, T. W. J., Job, D. E., Spencer, M. D., Whalley, H. C., Johnstone, E. C., &  
58 Lawrie, S. M. (2005). Empirical comparison of maximal voxel and non-isotropic  
59 adjusted cluster extent results in a voxel-based morphometry study of comorbid  
60 learning disability with schizophrenia. *Neuroimage*, 28(3), 544-552.  
Nelson, T. O., & Narens, L. (1990). Metamemory: A theoretical framework and new  
findings. *The psychology of learning and motivation*, 26, 125-141.

- 1  
2  
3 Nisbett, R. E., & Wilson, T. D. (1977). Telling more than we can know: Verbal reports  
4 on mental processes. *Psychological review*, 84(3), 231.
- 5  
6 Oishi, K., Zilles, K., Amunts, K., Faria, A., Jiang, H., Li, X., ... & Mori, S. (2008).  
7 Human brain white matter atlas: identification and assignment of common  
8 anatomical structures in superficial white matter. *Neuroimage*, 43(3), 447-457.
- 9  
10 Olson, I. R., & Berryhill, M. (2009). Some surprising findings on the involvement of the  
11 parietal lobe in human memory. *Neurobiology of learning and memory*, 91(2),  
12 155-165.
- 13  
14 Oouchi, H., Yamada, K., Sakai, K., Kizu, O., Kubota, T., Ito, H., et al. (2007). Diffusion  
15 anisotropy measurement of brain white matter is affected by voxel size:  
16 underestimation occurs in areas with crossing fibers. *American Journal of*  
17 *Neuroradiology*, 28(6), 1102-1106.
- 18  
19 Overgaard, M., & Sandberg, K. (2012). Kinds of access: different methods for report  
20 reveal different kinds of metacognitive access. *Philosophical Transactions of the*  
21 *Royal Society B: Biological Sciences*, 367(1594), 1287-1296.
- 22  
23 Pannu, J. K., & Kaszniak, A. W. (2005). Metamemory experiments in neurological  
24 populations: a review. *Neuropsychol Rev*, 15(3), 105-130.
- 25  
26 Ridderinkhof, K. R., Ullsperger, M., Crone, E. A., & Nieuwenhuis, S. (2004). The role of  
27 the medial frontal cortex in cognitive control. *Science Signaling*, 306(5695), 443.
- 28  
29 Rushworth, M. F., Behrens, T. E., & Johansen-Berg, H. (2006). Connection patterns  
30 distinguish 3 regions of human parietal cortex. *Cereb Cortex*, 16(10), 1418-1430.
- 31  
32 Schmahmann, J. D., Pandya, D. N., Wang, R., Dai, G., D'Arceuil, H. E., de Crespigny, A.  
33 J., et al. (2007). Association fibre pathways of the brain: parallel observations  
34 from diffusion spectrum imaging and autoradiography. *Brain*, 130(3), 630-653.
- 35  
36 Schmahmann, J. D., Smith, E. E., Eichler, F. S., & Filley, C. M. (2008). Cerebral white  
37 matter. *Annals of the New York Academy of Sciences*, 1142(1), 266-309.
- 38  
39 Schnyer, D. M., Verfaellie, M., Alexander, M. P., LaFleche, G., Nicholls, L., & Kaszniak,  
40 A. W. (2004). A role for right medial prefrontal cortex in accurate feeling-of-  
41 knowing judgments: evidence from patients with lesions to frontal cortex.  
42 *Neuropsychologia*, 42, 957-966.
- 43  
44 Schooler, J., & Schreiber, C. A. (2004). Experience, meta-consciousness, and the paradox  
45 of introspection. *Journal of consciousness studies*, 11(7-8), 7-8.
- 46  
47 Schooler, J. W. (2002). Re-representing consciousness: Dissociations between experience  
48 and meta-consciousness. *Trends in cognitive sciences*, 6(8), 339-344.
- 49  
50 Schooler, J. W., Reichle, E. D., & Halpern, D. V. (2004). Zoning out while reading:  
51 Evidence for dissociations between experience and metacognition. *Thinking*  
52 *and seeing: Visual metacognition in adults and children*, 203-226.
- 53  
54 Schooler, J. W., Smallwood, J., Christoff, K., Handy, T. C., Reichle, E. D., & Sayette, M.  
55 A. (2011). Meta-awareness, perceptual decoupling and the wandering mind.  
56 *Trends in cognitive sciences*, 15(7), 319-326.
- 57  
58 Segonne, F., Dale, A. M., Busa, E., Glessner, M., Salat, D., Hahn, H. K., et al. (2004). A  
59 hybrid approach to the skull stripping problem in MRI. *Neuroimage*, 22(3), 1060-  
60 1075.
- 61  
62 Seltzer, B., & Pandya, D. (1984). Further observations on parieto-temporal connections  
63 in the rhesus monkey. *Experimental Brain Research*, 55(2), 301-312.

- 1  
2  
3 Shimamura, A. P. (2000). The role of the prefrontal cortex in dynamic filtering.  
4 *Psychobiology*, 28(2), 207-218.
- 5  
6 Simons, J. S., Peers, P. V., Mazuz, Y. S., Berryhill, M. E., & Olson, I. R. (2010).  
7 Dissociation between memory accuracy and memory confidence following  
8 bilateral parietal lesions. *Cerebral Cortex*, 20(2), 479-485.
- 9  
10 Smallwood, J., McSpadden, M., & Schooler, J. W. (2008). When attention matters: The  
11 curious incident of the wandering mind. *Memory & Cognition*, 36(6), 1144-1150.
- 12  
13 Song, C., Kanai, R., Fleming, S. M., Weil, R. S., Schwarzkopf, D. S., & Rees, G. (2011).  
14 Relating inter-individual differences in metacognitive performance on different  
15 perceptual tasks. *Consciousness and Cognition*, 20(4), 1787-1792.
- 16  
17 Swets, J. A. (1986). Form of empirical ROCs in discrimination and diagnostic tasks:  
18 implications for theory and measurement of performance. *Psychol Bull*, 99(2),  
19 181-198.
- 20  
21 Terrace, H. S., & Metcalf, J. S. (2004). *The Missing Link in Cognition: Origins of Self-  
22 Reflective Consciousness: Origins of Self-Reflective Consciousness*. Oxford  
23 University Press.
- 24  
25 Tuch, D. S. (2004). Q<sub>1</sub>ball imaging. *Magnetic Resonance in Medicine*, 52(6), 1358-1372.
- 26  
27 Vilberg, K., & Rugg, M. (2008). Memory retrieval and the parietal cortex: a review of  
28 evidence from a dual-process perspective. *Neuropsychologia*, 46(7), 1787.
- 29  
30 Vilberg, K. L., Moosavi, R. F., & Rugg, M. D. (2006). The relationship between  
31 electrophysiological correlates of recollection and amount of information  
32 retrieved. *Brain Research*, 1122(1), 161.
- 33  
34 Vincent, J. L., Snyder, A. Z., Fox, M. D., Shannon, B. J., Andrews, J. R., Raichle, M. E.,  
35 et al. (2006). Coherent spontaneous activity identifies a hippocampal-parietal  
36 memory network. *J Neurophysiol*, 96(6), 3517-3531.
- 37  
38 Vos, S. B., Jones, D. K., Viergever, M. A., & Leemans, A. (2011). Partial volume effect  
39 as a hidden covariate in DTI analyses. *Neuroimage*, 55(4), 1566-1576.
- 40  
41 Wagner, A. D., Shannon, B. J., Kahn, I., & Buckner, R. L. (2005). Parietal lobe  
42 contributions to episodic memory retrieval. *Trends Cogn Sci*, 9(9), 445-453.
- 43  
44 Wedeen, V. J., Hagmann, P., Tseng, W. Y. I., Reese, T. G., & Weisskoff, R. M. (2005).  
45 Mapping complex tissue architecture with diffusion spectrum magnetic resonance  
46 imaging. *Magnetic Resonance in Medicine*, 54(6), 1377-1386.
- 47  
48 Wheeler, M. E., & Buckner, R. L. (2004). Functional-anatomic correlates of  
49 remembering and knowing. *Neuroimage*, 21(4), 1337-1349.
- 50  
51 Wilson, M. (1988). MRC Psycholinguistic Database: Machine-usable dictionary, version  
52 2.00. *Behavior Research Methods, Instruments, & Computers*, 20(1), 6-10.
- 53  
54 Worsley, K., Andermann, M., Koulis, T., MacDonald, D., & Evans, A. (1999). Detecting  
55 changes in nonisotropic images. *Human brain mapping*, 8(2-3), 98-101.
- 56  
57 Yeh, F. C., Tang, P. F., & Tseng, W. Y. I. (2013a). Diffusion MRI connectometry  
58 automatically reveals affected fiber pathways in individuals with chronic stroke.  
59 *NeuroImage: clinical*, 2, 912-921.
- 60  
61 Yeh, F.-C., Verstynen, T. D., Wang, Y., Fernández-Miranda, J. C., & Tseng, W.-Y. I.  
62 (2013b). Deterministic Diffusion Fiber Tracking Improved by Quantitative  
63 Anisotropy. *PloS one*, 8(11), e80713.
- 64  
65 Yeh, F.-C., Wedeen, V. J., & Tseng, W.-Y. (2010). Generalized-Sampling Imaging.  
66 *Medical Imaging, IEEE Transactions on*, 29(9), 1626-16.



**Table 1. White matter microstructure associated with metacognitive ability in memory and perception domains**

Region	Volume (mm <sup>3</sup> )	Peak MNI			Z-value
		X	Y	Z	
<i>Quantitative Anisotropy (QA)</i>					
Memory ( $M_{ratio}$ )					
R inferior parietal lobule WM	93	42	-48	27	3.85
Perception ( $A_{roc}$ )					
No suprathreshold clust.	N/A	N/A			N/A
<i>Generalized Fractional Anisotropy (GFA)</i>					
Memory ( $M_{ratio}$ )					
No suprathreshold clust.	N/A	N/A			N/A
Perception ( $A_{roc}$ )					
R anterior cingulate cortex WM	78	12	30	33	3.48

\*All clusters significant at  $p < .05$ , FWE corrected (height threshold,  $p < .005$ ).

For Review Only

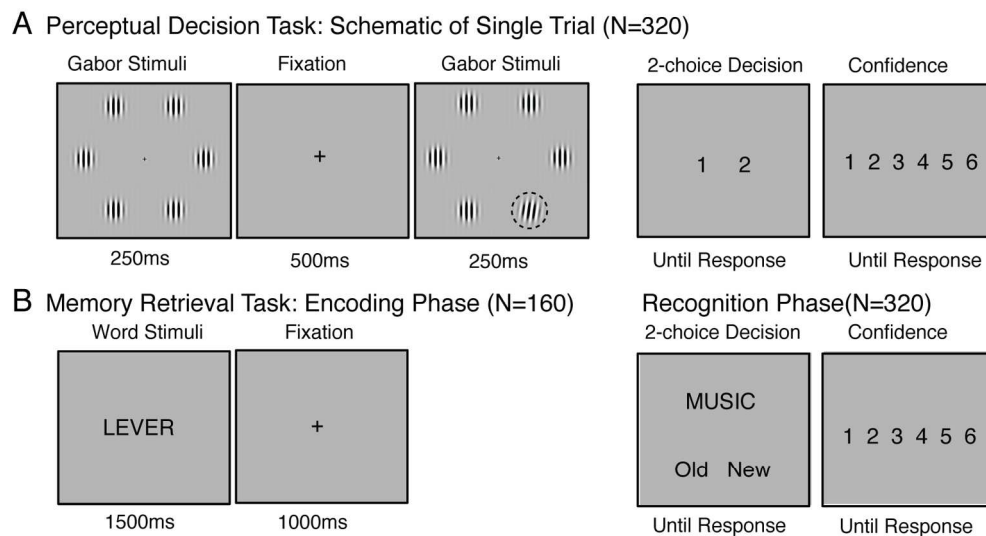


Figure 1. Experimental paradigm. Participants completed 2 tasks in a counter-balanced order. A, Perceptual Discrimination Task. Each trial (N=320) consisted of a visual display of 6 Gabor gratings, followed by an interstimulus interval (ISI) of 500ms, followed by a second visual display of 6 Gabor gratings. In one of the two displays, the orientation of one randomly selected Gabor patch was tilted slightly from the vertical axis (indicated here with a dashed circle that was not present in the actual display). The orientation angle of this pop-out Gabor was adjusted using a 2-up 1-down adaptive staircase procedure. Participants made unspeeded 2-choice discrimination judgments as to whether the “pop-out” Gabor occurred in either the first or second stimulus display, and then rated their confidence in the accuracy of their response on a scale of 1 (low confidence) to 6 (high confidence). B, Memory Retrieval Task. The memory task consisted of a classic verbal recognition memory paradigm. During encoding, participants viewed 160 words randomly selected from a set of 320 words. During recognition, participants were presented with each word from the full list of stimuli in a random order (half of which were presented during encoding and half of which were new), and were asked to make unspeeded 2-choice discrimination judgments as to whether the stimulus was old or new, and then rated their confidence in their response.

161x91mm (300 x 300 DPI)

1  
2  
3  
4  
5  
6  
7  
8  
9  
10  
11  
12  
13  
14  
15  
16  
17  
18  
19  
20  
21  
22  
23  
24  
25  
26  
27  
28  
29  
30  
31  
32  
33  
34  
35  
36  
37  
38  
39  
40  
41  
42  
43  
44  
45  
46  
47  
48  
49  
50  
51  
52  
53  
54  
55  
56  
57  
58  
59  
60

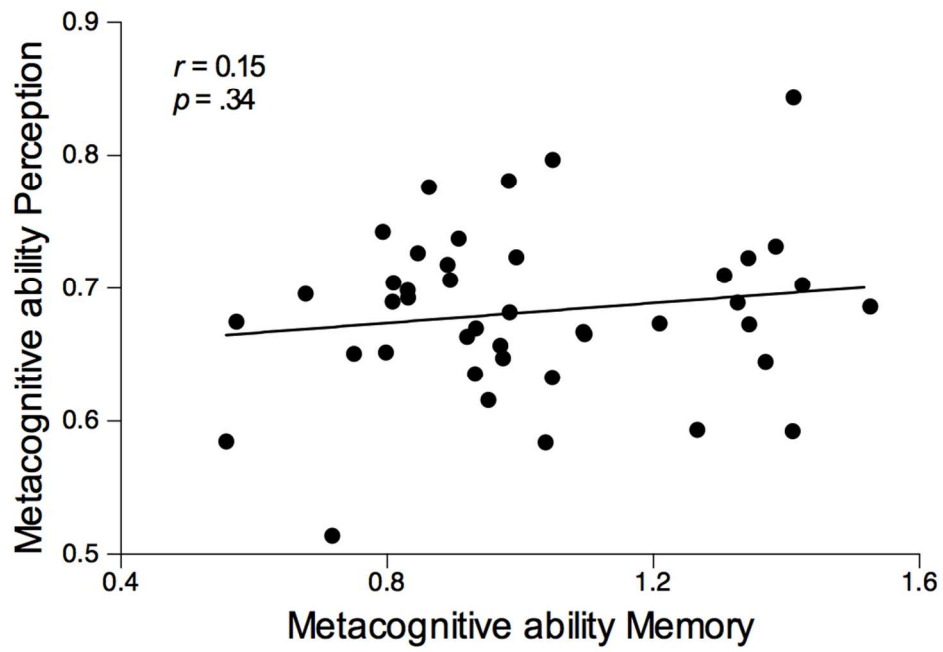


Figure 2. Scatterplot of zero-order correlation between metacognitive ability for perceptual decisions (Aroc) and mnemonic judgments (Mratio) [ $r(42) = 0.15$ ,  $p = 0.34$ ].  
95x64mm (300 x 300 DPI)

Pre-View Only

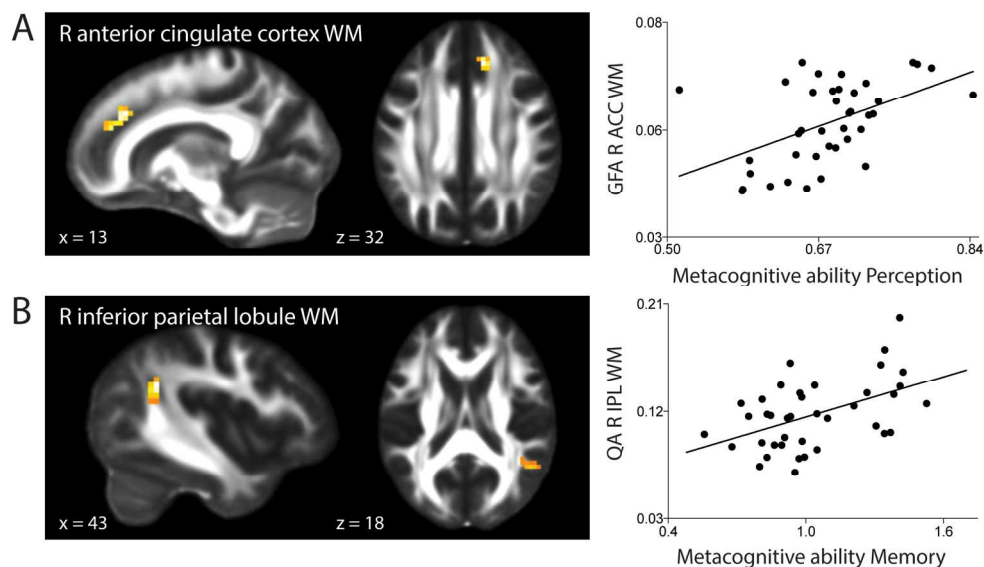


Figure 3. White matter microstructure (diffusion anisotropy) associated with metacognitive ability for memory and perception. A, Metacognitive accuracy for perceptual decisions is associated with increased GFA in the white matter underlying the right anterior cingulate cortex (ACC). B, Metacognitive accuracy for memory retrieval is associated with increased QA in the white matter extending into the inferior parietal lobule (IPL). All clusters significant at  $p < .05$ , FWE corrected (height threshold,  $p < .005$ ). Scatterplots show the correlations between metacognitive accuracy scores and median anisotropy values of significant clusters. R: right, WM: white matter; QA: quantitative anisotropy, GFA: generalized fractional anisotropy. 163x92mm (300 x 300 DPI)

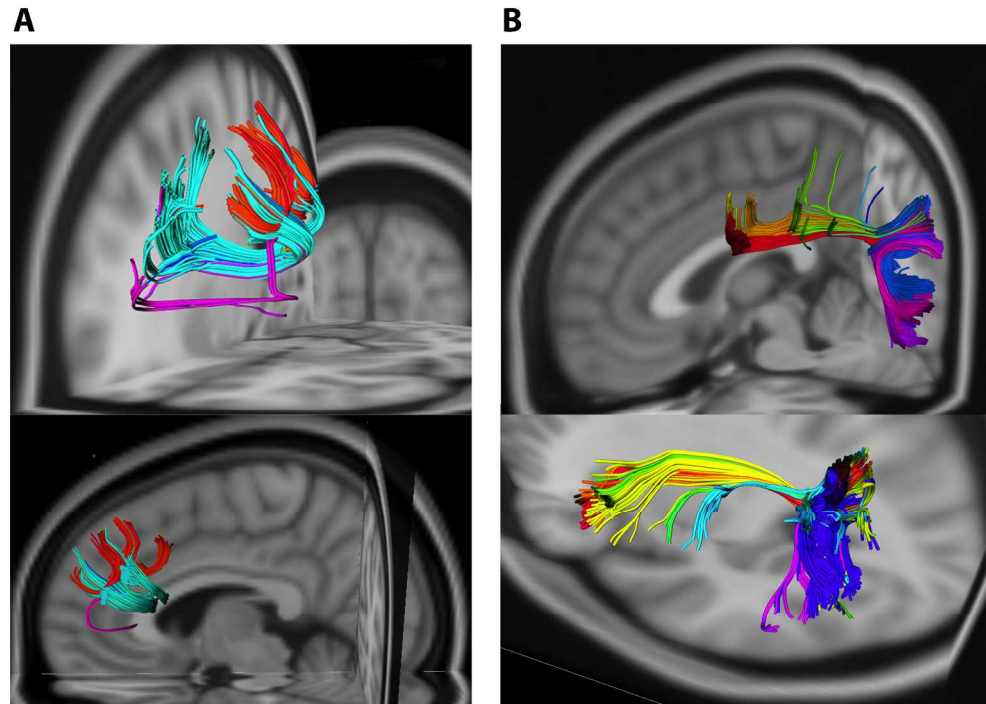


Figure 4. Tractography of ACC and IPL white matter regions in a representative subject. A, The right ACC white matter cluster connected right aSTG to the right caudal ACC (orange/red), right aSTG to left aSTG (turquoise), and right aSTG to left caudal ACC (purple). B, The right IPL white matter cluster contained prominent tracts connecting IPL to MFG (orange/red), IPL to precentral gyrus (yellow), IPL to postcentral gyrus (green), IPL to superior/middle/inferior temporal lobe (purple), and within-area connections in IPL (dark blue) and supramarginal gyrus (light blue). Images are displayed in radiological convention: the left side of the brain reflects the right hemisphere.

1027x732mm (72 x 72 DPI)